Bull Math Biol (2015) 77:1886–1908
DOI 10.1007/s11538-015-0108-2

Society for Mathematical Biology

ORIGINAL ARTICLE

Revisiting the Stability of Spatially Heterogeneous Predator–Prey Systems Under Eutrophication

J. Z. Farkas[1] · **A. Yu. Morozov**[2] · **E. G. Arashkevich**[3] · **A. Nikishina**[3]

Received: 22 February 2015 / Accepted: 16 September 2015 / Published online: 24 September 2015

Abstract We employ partial integro-differential equations to model trophic interaction in a spatially extended heterogeneous environment. Compared to classical reaction–diffusion models, this framework allows us to more realistically describe the situation where movement of individuals occurs on a faster time scale than on the demographic (population) time scale, and we cannot determine population growth based on local density. However, most of the results reported so far for such systems have only been verified numerically and for a particular choice of model functions, which obviously casts doubts about these findings. In this paper, we analyse a class of integro-differential predator–prey models with a highly mobile predator in a heterogeneous environment, and we reveal the main factors stabilizing such systems. In particular, we explore an ecologically relevant case of interactions in a highly eutrophic environment, where the prey carrying capacity can be formally set to 'infinity'. We

Electronic supplementary material The online version of this article (doi:10.1007/s11538-015-0108-2) contains supplementary material, which is available to authorized users.

✉ A. Yu. Morozov
am379@leicester.ac.uk

J. Z. Farkas
jozsef.farkas@stir.ac.uk

E. G. Arashkevich
aelena@ocean.ru

A. Nikishina
anastasia.nikishina@gmail.com

1 Division of Computing Science and Mathematics, University of Stirling, Stirling FK9 4LA, UK

2 Department of Mathematics, University of Leicester, Leicester LE1 7RH, UK

3 Shirshov Institute of Oceanology, Moscow 117851, Russia

investigate two main scenarios: (1) the spatial gradient of the growth rate is due to abiotic factors only, and (2) the local growth rate depends on the global density distribution across the environment (e.g. due to non-local self-shading). For an arbitrary spatial gradient of the prey growth rate, we analytically investigate the possibility of the predator–prey equilibrium in such systems and we explore the conditions of stability of this equilibrium. In particular, we demonstrate that for a Holling type I (linear) functional response, the predator can stabilize the system at low prey density even for an 'unlimited' carrying capacity. We conclude that the interplay between spatial heterogeneity in the prey growth and fast displacement of the predator across the habitat works as an efficient stabilizing mechanism. These results highlight the generality of the stabilization mechanisms we find in spatially structured predator–prey ecological systems in a heterogeneous environment.

Keywords Spatially structured populations · Partial integro-differential equations · Stability · Paradox of enrichment · Top-down control

1 Introduction

Understanding top-down control in food webs has been always a focus of theoretical ecology, and revealing potential mechanisms which stabilize predator–prey/resource–consumer interactions in ecosystems with a high degree of eutrophication (i.e. ecosystems that are high in nutrients) is a particularly challenging problem (Rosenzweig 1971; Oaten and Murdoch 1975; Armstrong 1994; Jansen 1995; Abrams and Walters 1996; Briggs and Hoopes 2004; Morozov et al. 2013). Classical theory predicts that a generic predator–prey system will be highly unstable under eutrophic conditions and is expected to exhibit large-amplitude oscillations of species densities which will eventually result in population collapse and extinction (Rosenzweig 1971; Gilpin 1972). However, these theoretical conclusions are often at odds with reality, since there exist a large number of examples of ecosystems in which the species densities remain low despite a high nutrient supply (Chavez et al. 1990; Cullen et al. 1992; Boyd 2002; Jensen and Ginzburg 2005; Roy and Chattopadhyay 2007). Various mechanisms have been proposed to explain such stability of predator–prey interactions in eutrophic environments. In particular, it has been suggested that this could be due to interplay between structuring within the prey population according to vulnerability or nutrition properties and active food selectivity of the predator (prey switching) (Abrams and Walters 1996; Genkai-Kato and Yamamura 1999; Mougi and Nishimura 2007; Morozov et al. 2007, 2013; Farkas and Morozov 2014). However, stabilization mechanisms of this kind cease working for unstructured populations, so a natural question is whether efficient top-down control is possible for a population of identical prey individuals.

Spatial heterogeneity of the environment and a non-homogeneous distribution of individuals across the habitat has been suggested to be an important factor promoting top-down control and preventing species extinction (Jansen 1995; Nisbet et al. 1997; Poggiale and Auger 2004; Briggs and Hoopes 2004; Petrovskii et al. 2004). In recent model studies of planktonic systems with a high nutrient supply, it was shown

that interplay between the gradient of light in the water column and fast vertical displacement of herbivorous zooplankton can stabilize the system even for an unlimited nutrient stock (Morozov et al. 2011; Lewis et al. 2013). The works cited implement a modelling approach which differs from the classical reaction–diffusion framework in several important ways. In particular, the new approach allows for different time scales for the population growth rate of prey and its predator and also takes into account the fact that the rate at which predator disperses across the habitat can be substantially faster than its characteristic demographic scale. For example, zooplankton herbivores can quickly move vertically along the entire habitat (in the euphotic part of water column) a large number of times between reproduction events; thus, we cannot assign an organism to a particular spatial location (Cottier et al. 2006), as in the case of reaction–diffusion models. Thus, we should describe the predator population as a whole in terms of the total population size, while still taking into account non-homogeneity of the distribution of predator individuals across the habitat when considering grazing of the prey at each particular location. Ecologically similar scenarios can be found in a large number of other ecosystems when modelling, for instance, interactions between terrestrial herbivorous mammals and grass, zooplankton and fish, insects and birds, insects and their parasitoids, acarine predator–prey systems and even between fish population and fishing boats (Milinski 1979; Godin and Keenleyside 1984; Lodge et al. 1988; Kacelnik et al. 1992; Begon et al. 2005; Nachman 2006; Auger et al. 2010).

Modelling predator–prey interaction in a spatially heterogeneous habitat, where an exact location of individuals on a demographic time scale cannot be properly assigned, requires the implementation of *partial integro-differential equations*. However, the complexity of this framework makes it rather difficult to treat the model analytically: all previous findings have been obtained by direct numerical simulations of the equations for particular parameterizations of the model ingredients (Morozov et al. 2011; Lewis et al. 2013). This, obviously, cannot be considered as a rigorous proof of stabilization of the system. Moreover, the results can strongly depend on the choice of the per capita population growth rate, which in the previous studies was considered to be an exponential function modelling light attenuation with depth (Morozov et al. 2011; Lewis et al. 2013). Finally, we should say that the integro-differential equations in Morozov et al. (2011) and Lewis et al. (2013) differ significantly from those used in the modelling of physiologically structured populations, see for example Cushing (1998) and Farkas and Hagen (2007). For instance, the model we develop here does not contain a transport term as standard physiologically structured models do.

In this paper, we revisit the previous results on stabilization for a class of integro-differential predator–prey models and explore the main factors assuring efficient top-down control. We analytically obtain criteria for the existence of a positive stationary state assuring the coexistence of both species for an arbitrary gradient of resource distribution across the environment. Then, we investigate the stability of the coexistence equilibrium and derive a general characteristic equation, which governs the stability of the system. We analytically show that in the case that there is no saturation in the functional response (i.e. Holling type I response), the predator is able to stabilize the system at low prey density even for an 'unlimited' carrying capacity. We study how the size of the habitat and the spatial gradient of the prey growth affects stabilization in the system. We explore two ecologically relevant scenarios: (1) the case when the

spatial gradient of the growth rate of the prey is due to abiotic factors only, and (2) the case where the growth rate of the prey is affected by the surrounding density of the population itself (e.g. effects of self-shading). We find that, interestingly, in case (1) the trophic control of the prey is not possible when the population size of the predator varies slowly, whereas in case (2) the predator can efficiently suppress the population growth even without changing its own population size.

2 Modelling Framework and Biological Rationale

The general predator–prey model with a highly mobile predator is described by the following system of partial integro-differential equations (Morozov et al. 2011).

$$\frac{\partial p}{\partial t}(h,t) = D\frac{\partial^2 p}{\partial h^2}(h,t) + R(h,p(h,t))p(h,t) - f(p(h,t))z(h,t), \quad p(h,0) = p_0(h), \tag{1}$$

$$\frac{\mathrm{d}Z}{\mathrm{d}t}(t) = \frac{k}{H}\int_0^H f(p(h,t))z(h,t)\mathrm{d}h - mZ(t), \quad Z(0) = Z_0, \tag{2}$$

$$Z(t) = \frac{1}{H}\int_0^H z(h,t)\mathrm{d}h, \quad P(t) = \frac{1}{H}\int_0^H p(h,t)\mathrm{d}h. \tag{3}$$

In the model above, $p(h,t)$ and $z(h,t)$ denote the densities of prey and predator at time t and at spatial location h, respectively; H is the overall size of the habitat; hence, $P(t)$ and $Z(t)$ are the average densities of the species at time t, while p_0 and Z_0 denote the initial conditions. The first term in the right-hand side of (1) describes the dispersal of prey across the habitat due to diffusion; R is the function (or functional, in general) describing the local per capita growth rate of the prey; f is the local functional response of the predator. The parameters k and m denote the food efficiency of the predator and its mortality rate, respectively. In the case where we model plankton interactions, h is the vertical coordinate from the water surface and H is the overall depth of the euphotic zone.

Here, we impose zero flux boundary conditions $\frac{\partial p}{\partial h} = 0$ at $h = 0$ and $h = H$.

The integro-differential framework (1)–(3) is quite different from the conventional reaction–diffusion modelling setting. Here, we consider that the predator movement occurs on a much faster time scale than both the prey movement and the population dynamics and assume that the predator can quickly move to any part of the habitat. Thus, we cannot assign a particular spatial location to an individual within the predator population, since organisms constantly change their locations. The framework still allows us to consider the instantaneous spatial distribution of the predator population $z(h,t)$. Note that Eqs. (1)–(3) do not uniquely specify $z(h,t)$ based on the knowledge of $Z(t)$, so we need to impose some further assumptions. A number of empirical observations suggest that the relative distribution of predator between patches often follows the relative abundance of food, which is described by

$$z(h,t) = \frac{p(h,t)}{P(t)}Z(t). \tag{4}$$

The above proportion-based parametrization may not be realistic since it does not take into account possible interference between predators (Murdoch et al. 1992). However, in a large number of study cases, see for example Milinski (1979), Godin and Keenleyside (1984), Kacelnik et al. (1992), Larsson (1997) and Nachman (2006), we can still reasonably well approximate the instantaneous spatial distribution of predator across the food patches by (4). For instance, the distribution of herbivorous zooplankton in the water column often follows that of phytoplankton, see for example Lampert (2005) and Morozov et al. (2011).

Figure 1a shows a typical example of the relative distribution of the biomass of phytoplankton (prey) and herbivorous zooplankton (predator) in different layers of the vertical water column in the euphotic zone of the sea. Here, we split the water column into a number of layers and plot the values of the spatially averaged biomass of p and z in each layer divided by the overall average biomass across the entire column. The data were recently collected at 12 stations in the Black Sea for various seasons (2007–2013); further details on obtaining the samples are provided in electronic Appendix 1. The figure presents both night and day observations. For the night observation (open circles), one can see that the data can be roughly described by the straight line with slope approximately equal to 1; thus, the basic assumption (4) holds (standard linear regression gives $R^2 = 0.85$ and the slope of the fitting line as 0.96).

The major difference between the night and the day patterns is that the vertical distribution of zooplankton substantially varies due to the phenomenon of regular daily vertical migration: during the day time zooplankton is mainly located in deep layers to avoid predation by higher visual predators (e.g. fish) and ascend to upper layers at night (Ohman 1990). Note that daytime feeding activity of herbivorous zooplankton is usually low and most of the food is consumed during the night time (Bollens and Frost 1989).

Figure 1b provides examples of vertical distributions of species and the daily zooplankton migration pattern. One can see that the vertical distribution of zooplankton is highly variable throughout the 24-h period. Moreover, zooplankton usually exhibit fast short-term unsynchronized migrations (Cottier et al. 2006), by permanently descending and ascending over smaller distances (10–20 m). Thus, we cannot assign a particular location to an individual zooplankton, and we can use the integro-differential framework with an instantaneous distribution of the predator. We should note that model (1)–(3) describes the organisms averaged over the day, and therefore excluding daily migration patterns. Finally, Fig. 1b also provides the profile of chlorophyll a through the column, which is a proxy of the distribution of phytoplankton. Its complicated structure is due to high heterogeneity in the distribution of the vital resources: light and nutrients (phosphorous and nitrogen) through the column, which potentially translates into a complicated relation $r(h)$ (cf. Ryabov and Blasius 2011).

We consider that the local functional response is given by the Holling type II function (Holling 1959; Gentleman et al. 2003)

$$f(p) = \alpha \frac{p}{1 + p\beta}, \tag{5}$$

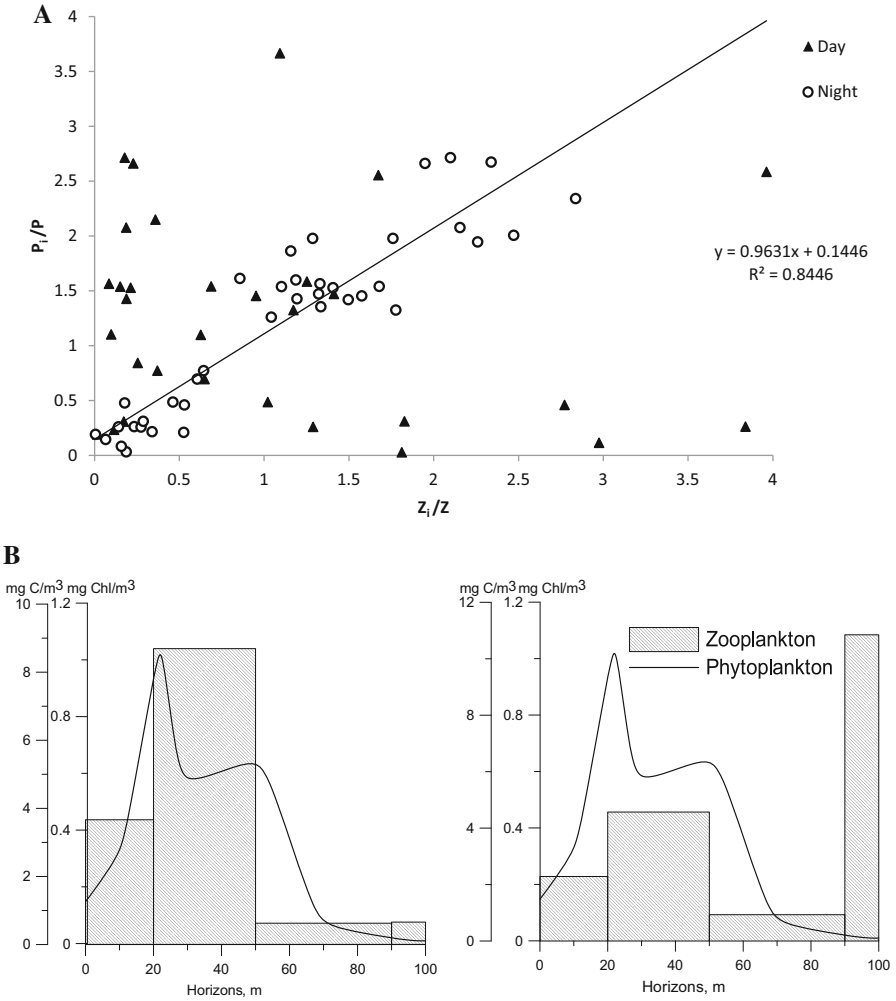

Fig. 1 **a** Relative distribution of phytoplankton and zooplankton biomass across the water column collected at 12 stations in the Black Sea. Details on plankton sampling are provided in electronic Appendix 1. For each station, the whole euphotic zone is split into a number of layers. Figure shows the relative phytoplankton biomass plotted against the relative zooplankton biomass in the same layer. Here, P_i and Z_i are the average densities of species in layer i; P and Z are the overall average densities, **b** typical example of vertical distribution of zooplankton (mg C/m^3) and phytoplankton (mg Chl/m^3) during night (*left panel*) and daytime (*right panel*) collected at station #5. The profile of phytoplankton distribution is averaged over 24 h. High variation in zooplankton distribution through the day is due to the diel vertical migration (for more explanation see text)

where the parameters α and β denote the attack rate and the inverse saturation food density, respectively. In the limiting case when $\beta = 0$ the functional response becomes linear or Holling type I response. Here, we intentionally implement a concave downwards (i.e. non-sigmoidal) functional response, which is a destabilizing factor in

predator–prey models in general, see for example Rosenzweig (1971) and Gilpin (1972).

For the sake of simplicity, we neglect the effect of diffusion of the prey by setting $D = 0$. In Sect. 4, we shall briefly address the effect that prey diffusion has on the results.

Finally, we need to specify the growth function R. Since we model eutrophic conditions, we consider that this function does not depend on the variation of nutrient concentration. We shall explore two main scenarios: (1) the per capita growth rate is a function of the abiotic environment only, i.e. it is a local function $R = r(h)$ and (2) the per capita growth rate depends on the population density distribution in some parts of the environment $R = R(h, p)$, i.e. it is a non-local term. In the latter case, we have a functional, i.e. a function which depends on another function characterizing the overall spatial distribution of p. Note that in both cases, we neglect natural mortality of the prey compared to the predation rate.

In case (1), the equations read (Model 1)

$$\frac{\partial p}{\partial t}(h,t) = r(h)p(h,t) - \frac{1}{P(t)}\alpha\frac{p^2(h,t)}{1+\beta p(h,t)}Z(t), \quad p(h,0) = p_0(h), \tag{6}$$

$$\frac{\mathrm{d}Z}{\mathrm{d}t}(t) = k\frac{Z(t)}{HP(t)}\alpha\int_0^H \frac{p^2(h,t)}{1+\beta p(h,t)}\mathrm{d}h - mZ(t), \quad Z(0) = Z_0. \tag{7}$$

For the moment, we do not specify the function r. We only assume that it is a smooth and non-negative function.

In case (2), we shall investigate the particular scenario of self-shading in the population. In this complex scenario, the supply of a resource such as light decreases in space via a function of the local population density. In planktonic communities, this may be shading of light for phytoplankton residing in deeper layers by the organisms dwelling in upper layers. For a non-planktonic system, this may be, for instance, a gradual depletion of a nutrient as it flows through part of the environment occupied by the prey and is gradually consumed by the organisms. In this case, the local rate of decrease in resource density can be assumed to be a function of the density of consumers. It is natural to assume that the available resource quantity is a decreasing function of the total number of consumers $\int_0^h p(x,t)\mathrm{d}x$ that are above/upstream an individual at depth/point h. In particular, we assume that the quantity of the available resource is an exponentially decreasing function of the number of consumers that contribute to the shading.

The equations read (Model 2)

$$\frac{\partial p}{\partial t}(h,t) = r_0\exp\left(-\nu\int_0^h p(x,t)\mathrm{d}x\right)p(h,t) - \frac{1}{P(t)}\alpha\frac{p^2(h,t)}{1+\beta p(h,t)}Z(t),$$
$$p(h,0) = p_0(h), \tag{8}$$

$$\frac{\mathrm{d}Z}{\mathrm{d}t}(t) = k\frac{Z(t)}{HP(t)}\alpha\int_0^H \frac{p^2(h,t)}{1+\beta p(h,t)}\mathrm{d}h - mZ(t), \quad Z(0) = Z_0, \tag{9}$$

where ν is the coefficient of self-shading. In both of the models above the average densities, $P(t)$ and $Z(t)$ are given by Eq. (3).

In this paper, we are mostly interested in the existence and stability of the positive stationary state of (6)–(7) and (8)–(9). It is worth mentioning that a spatially homogeneous predator–prey model (1)–(3) with perfect mixing (i.e. for $r(h) = const$ and $z(h) = const$) will be globally unstable (Bazykin 1998); thus, the main question is whether it is possible to stabilize this system by introducing spatial heterogeneity (i.e. structuring the population) and allowing a non-homogeneous distribution of predators. It is also worth noting that the term describing prey growth in Eq. (8) has infinite dimensional nonlinearity, and that structured population models with such nonlinearity are notoriously difficult to analyse, see for example Calsina and Farkas (2012) and Farkas and Hagen (2009).

3 Results

3.1 Model 1: The Local Growth Rate of the Prey is a Function of Abiotic Factors Only

3.1.1 Existence of a Non-trivial (Coexistence) Steady State

We look for a strictly positive steady state (p_*, Z_*) of model (6)–(7). We assume that r is a strictly positive continuous function with

$$\max_{h\in[0,H]}\{r(h)\} = r_M.$$

We characterize the existence of the positive steady state in the following proposition.

Proposition 3.1 *Assume that*

$$\alpha k > m\beta \tag{10}$$

holds. Then, model (6)–(7) *has a unique positive steady state.*

Proof The steady-state equations read

$$r(h) = \alpha\frac{Z_*}{P_*}\frac{p_*(h)}{1+\beta p_*(h)}, \quad h\in[0,H], \tag{11}$$

$$Z_* = \frac{\alpha k}{mH}\int_0^H \frac{p_*^2(h)}{1+\beta p_*(h)}\mathrm{d}h, \tag{12}$$

$$P_* = \frac{1}{H}\int_0^H p_*(h)\mathrm{d}h. \tag{13}$$

For positive values (P_*, Z_*) which satisfy

$$\alpha Z_* > \beta r_M P_*, \tag{14}$$

we obtain from Eq. (11)

$$p_*(h) = \frac{r(h)}{\alpha \frac{Z_*}{P_*} - r(h)\beta}, \quad h \in [0, H]. \tag{15}$$

We then substitute the steady state p_* given by formula (15) into Eqs. (12)–(13). After simplification, we obtain:

$$P_* = \frac{1}{H} \int_0^H \frac{r(h)}{\alpha \frac{Z_*}{P_*} - r(h)\beta} \mathrm{d}h, \tag{16}$$

$$Z_* = \frac{k}{mH} \int_0^H \frac{r^2(h)}{\alpha \frac{Z_*}{P_*} - r(h)\beta} \mathrm{d}h. \tag{17}$$

From Eq. (17), we obtain:

$$\begin{aligned} Z_* &= \frac{k}{mH} \int_0^H \left[-\frac{1}{\beta} \frac{\alpha \frac{Z_*}{P_*} - r(h)\beta}{\alpha \frac{Z_*}{P_*} - r(h)\beta} r(h) + \frac{1}{\beta} \frac{\alpha \frac{Z_*}{P_*}}{\alpha \frac{Z_*}{P_*} - r(h)\beta)} r(h) \right] \mathrm{d}h \\ &= -\frac{k}{\beta m H} \int_0^H r(h) \mathrm{d}h + \frac{k}{m} \frac{\alpha Z_*}{\beta}, \end{aligned} \tag{18}$$

from which we obtain

$$Z_* = \frac{k}{\alpha k - m\beta} \frac{1}{H} \int_0^H r(h) \mathrm{d}h. \tag{19}$$

We substitute this expression into Eq. (16) to obtain

$$1 = \frac{1}{H} \int_0^H \frac{r(h)}{\frac{1}{H} \int_0^H r(h) \mathrm{d}h \frac{\alpha k}{\alpha k - m\beta} - r(h)\beta P_*} \mathrm{d}h =: F(P_*). \tag{20}$$

Also note that (14) together with (19) require the existence of a (unique) solution of (20) in the interval

$$\left(0, \frac{\alpha k}{\alpha k - m\beta} \frac{1}{\beta r_M} \frac{1}{H} \int_0^H r(h) \mathrm{d}h\right). \tag{21}$$

Note that $F(0) = \frac{\alpha k - m\beta}{\alpha k} < 1$, and that

$$F(P_*) \to +\infty, \quad \text{as} \quad P_* \to \left(\frac{\alpha k}{\alpha k - m\beta} \frac{1}{\beta r_M} \frac{1}{H} \int_0^H r(h) \mathrm{d}h \right)^-. \tag{22}$$

Hence, there is a solution of Eq. (20) in the required interval (21). It is also shown that on the interval (21), the function F is strictly monotonically increasing; hence, the solution is unique, and the proof is complete. □

Note that we may relax the assumption of strict positivity of r and allow it to vanish at some values of h. Then, Eq. (15) shows that the steady state p_* will also vanish at those values of h, but Proposition 3.1 still holds.

3.1.2 Stability of the Coexistence Steady State

The stability of the coexistence equilibrium is determined by the roots of a characteristic equation, which we derive in the current subsection. The linearization around the coexistence steady state (p_*, Z_*) of model (6)–(7) is computed as

$$\begin{aligned}\frac{\partial \Delta p}{\partial t}(h,t) &= r(h)\Delta p(h,t)\\ &\quad - \alpha\left(\frac{p_*^2(h)}{P_*(1+\beta p_*(h))}\Delta Z(t) - \frac{p_*^2(h)Z_*}{P_*^2(1+\beta p_*(h))}\Delta P(t)\right.\\ &\quad \left. + \frac{Z_* p_*(h)(2+\beta p_*(h))}{P_*(1+\beta p_*(h))^2}\Delta p(h,t)\right), \qquad (23)\\ \frac{\mathrm{d}\Delta Z}{\mathrm{d}t}(t) &= -m\Delta Z(t) + \frac{\alpha k}{HP_*}\Delta Z(t)\int_0^H \frac{p_*^2(h)}{1+\beta p_*(h)}\mathrm{d}h\\ &\quad - \frac{\alpha k Z_*}{HP_*^2}\Delta P(t)\int_0^H \frac{p_*^2(h)}{1+\beta p_*(h)}\mathrm{d}h\\ &\quad + \frac{\alpha k Z_*}{HP_*}\int_0^H \frac{p_*(h)(2+\beta p_*(h))}{(1+\beta p_*(h))^2}\Delta p(h,t)\mathrm{d}h,\\ &\quad \times \Delta P(t) = \frac{1}{H}\int_0^H \Delta p(h,t)\mathrm{d}h. \qquad (24)\end{aligned}$$

We look for the solution in the form of $\Delta p(h,t) = w(h)\exp(\lambda t)$ and $\Delta Z(t) = U\exp(\lambda t)$. This leads to the eigenvalue problem (W is the spatial average of w)

$$\begin{aligned}&\left(\lambda - r(h) + \alpha\frac{Z_*}{P_*}\frac{p_*(h)(2+\beta p_*(h))}{(1+\beta p_*(h))^2}\right)w(h)\\ &\quad = -\alpha\frac{p_*^2(h)}{P_*(1+\beta p_*(h))}U + \alpha\frac{Z_*}{P_*^2}\frac{p_*^2(h)}{1+\beta p_*(h)}W, \qquad (25)\\ &\lambda U = -mU\\ &\quad + \frac{\alpha k}{H}\int_0^H\left(\frac{p_*^2(h)}{P_*(1+\beta p_*(h))}U - \frac{p_*^2(h)Z_*}{P_*^2(1+\beta p_*(h))}W + \frac{Z_* p_*(h)(2+\beta p_*(h))}{P_*(1+\beta p_*(h))^2}w(h)\right)\mathrm{d}h. \qquad (26)\end{aligned}$$

Using (15), we recast Eq. (25) as follows

$$\left(\lambda + r(h)\left(1 - \frac{P_*}{Z_*}\frac{\beta}{\alpha}r(h)\right)\right)w(h) = \frac{r^2(h)}{\alpha Z_* - P_*\beta r(h)}W - \frac{P_* r^2(h)}{Z_*(\alpha Z_* - P_*\beta r(h))}U. \qquad (27)$$

Note that (14) implies that $\alpha Z_* - P_* r(h) > 0$, for $h \in [0, H]$. Next, we multiply equation (25) by $\frac{k}{H}$, then integrate it from 0 to H and add it to Eq. (26) to obtain:

$$\lambda k W + \lambda U = k\overline{W} - mU, \tag{28}$$

where

$$\overline{W} = \frac{1}{H}\int_0^H r(h)w(h)\mathrm{d}h. \tag{29}$$

We re-arrange equation (27) as

$$w(h) = \frac{r^2(h)}{k_1(\lambda, h)\,(\alpha Z_* - P_*\beta r(h))}W - \frac{r^2(h)}{k_1(\lambda, h)\,(\alpha Z_* - P_*\beta r(h))}\frac{P_*}{Z_*}U, \quad h \in [0, H], \tag{30}$$

where

$$k_1(\lambda, h) = \lambda + r(h)\left(1 - \frac{P_*}{Z_*}\frac{\beta}{\alpha}r(h)\right), \quad h \in [0, H].$$

Note that $k_1(\lambda, \cdot) \neq 0$ for $\lambda \in \mathbb{C}$, $\mathrm{Re}(\lambda) \geq 0$.

Next, we integrate equation (30) from 0 to H and divide by H to obtain

$$W = k_2(\lambda)W - k_2(\lambda)\frac{P_*}{Z_*}U, \tag{31}$$

where

$$k_2(\lambda) = \frac{1}{H}\int_0^H \frac{r^2(h)}{k_1(\lambda, h)\,(\alpha Z_* - P_*\beta r(h))}\mathrm{d}h.$$

We also multiply Eq. (30) by $\frac{r(h)}{H}$ and integrate from 0 to H to obtain

$$\overline{W} = k_3(\lambda)W - k_3(\lambda)\frac{P_*}{Z_*}U, \tag{32}$$

where

$$k_3(\lambda) = \frac{1}{H}\int_0^H \frac{r^3(h)}{k_1(\lambda, h)\,(\alpha Z_* - P_*\beta r(h))}\mathrm{d}h.$$

Next, we substitute into Eq. (28) the expression for $\overline{W}$ given by (32). This, together with Eq. (31), yields a homogeneous system of two equations for the variables (W, U) as follows.

$$\begin{aligned} 0 &= k\,(k_3(\lambda) - \lambda)\,W + \left(-k\frac{P_*}{Z_*}k_3(\lambda) - \lambda - m\right)U, \\ 0 &= (1 - k_2(\lambda))W + k_2(\lambda)\frac{P_*}{Z_*}U. \end{aligned} \tag{33}$$

For any value of $\lambda \in \mathbb{C}$ with $\mathrm{Re}(\lambda) \geq 0$ a non-trivial solution of system (33) yields a non-trivial solution w via Eq. (30). On the other hand, any eigenvalue λ with $\mathrm{Re}(\lambda) \geq 0$ necessarily satisfies Eq. (33) for same non-trivial (W, U).

We summarize our result in the following theorem:

Theorem 3.2 *The non-trivial steady state* (p_*, Z_*) *of model* (6)–(7) *is locally asymptotically stable if every solution* λ *of the characteristic equation below has negative real part.*

$$K(\lambda) := k\frac{P_*}{Z_*}k_3(\lambda) - k_2(\lambda)\left(\lambda\left(1 + k\frac{P_*}{Z_*}\right) + m\right) + \lambda + m = 0, \tag{34}$$

where k_2 *and* k_3 *are defined earlier. On the other hand, the steady state is unstable if there is at least one solution of* (34) *with positive real part.*

In general, the derived characteristic equation (34) is complicated and determining its roots might require extensive numerical simulations which might take as much time as directly solving the system of differential equations. However, this equation can be rather useful for construction of a Hopf bifurcation curve: one can set $\lambda = ib$ (b is a positive real number) and solve the resulting equation. In Sect. 4, we shall provide an example of construction of such a curve for a particular parametrization of the function r.

Using the characteristic equation above, we are able to address the stability of the system in the case when the demographic time scale of the predator is much slower than that of the prey. In this case, we can assume the population size of the predator to be constant. The result is given by the following remark.

Remark 3.3 The positive steady state (p_*, Z_*) is always unstable under perturbations in the first component (in the prey population) only. We consider perturbations in the p-subspace only. Perturbations in the first component only lead to the characteristic equation

$$\begin{aligned} 1 = k_2(\lambda) &= \frac{1}{H}\int_0^H \frac{r^2(h)}{k_1(\lambda, h)\,(\alpha Z_* - P_*\beta r(h))}\mathrm{d}h \\ &= \frac{1}{H}\int_0^H \frac{r^2(h)}{\left(\lambda + r(h)\left(1 - \frac{P_*}{Z_*}\frac{\beta}{\alpha}r(h)\right)\right)(\alpha Z_* - \beta P_* r(h))}\mathrm{d}h. \end{aligned} \tag{35}$$

It is shown that $k_2(0) > 1$, and clearly k_2 is a monotone decreasing function of λ for $\lambda > 0$. Also we have that $\lim_{\lambda\to+\infty} k_2(\lambda) = 0$; hence, there exists a unique positive eigenvalue, and the steady state is unstable.

Remark 3.4 Another important conclusion we may draw from (34) is that for a homogeneous environment (i.e. $r(h) \equiv const$), the system is always unstable provided $\beta > 0$, since all eigenvalues will have positive real parts (we do not show here the corresponding characteristic equation for the sake of simplicity).

3.1.3 Stability in the Special Case $\beta = 0$

Next, we investigate an important special case of (34) where we have a Holling type I functional response, i.e. there is no saturation rate in predation, $\beta = 0$. The characteristic equation reduces to

$$K(\lambda) = m + \lambda + \frac{P_*}{Z_*}\frac{k}{H}\int_0^H \frac{r^3(h)}{(\lambda + r(h))\alpha Z_*}\mathrm{d}h - \left(\lambda\left(1 + k\frac{P_*}{Z_*}\right) + m\right)\frac{1}{H}\int_0^H \frac{r^2(h)}{(\lambda + r(h))\alpha Z_*}\mathrm{d}h = 0, \tag{36}$$

which can be simplified by recalling the expressions for the stationary densities of species (16), (17) and (19). We obtain

$$K(\lambda) = m - \frac{2m\lambda}{\int_0^H r^2(h)\mathrm{d}h}\int_0^H \frac{r^2(h)\mathrm{d}h}{\lambda + r(h)} + \frac{(m+\lambda)\lambda}{\int_0^H r(h)\mathrm{d}h}\int_0^H \frac{r(h)\mathrm{d}h}{\lambda + r(h)} = 0, \tag{37}$$

Let us first consider the case of a small environment, i.e. small H. We use the Taylor expansion of (37). We assume that the derivative of $r(h)$ at $h = 0$ does not vanish: $r(h) \approx r_0 + Rh$, where $R \neq 0$. The characteristic equation becomes

$$0 = \frac{r_0 m + \lambda^2}{\lambda + r_0} + \frac{1}{2}r_0\gamma\lambda R\frac{m - \lambda}{(\lambda + r_0)^2}H - \frac{1}{12r_0}R^2\lambda\frac{r_0 m - 3\lambda m - 3r_0\lambda + \lambda^2}{(\lambda + r_0)^3}H^2 + O(H^3). \tag{38}$$

This expression can be re-written in the polynomial form ($\lambda \neq -r_0$) by dropping the term $O(H^3)$

$$0 = a_0 + a_1\lambda + a_2\lambda^2 + a_3\lambda^3 + a_4\lambda^4, \tag{39}$$

where $a_0 = r_0^3 m$, $a_1 = m(2r_0^2 - H^2R^2/12 + Hr_0R/2)$, $a_2 = mr_0 + r_0^2 - (r_0 - m)RH/2 - R^2(3m + 3r_0)H^2/(12r_0)$, $a_3 = 2r_0 - RH/2 - R^2H^2/(12r_0)$, $a_4 = 1$.

We use the Routh–Hurwitz stability criterion for the coefficients of the above polynomial: $a_n > 0, a_2a_3 > a_4a_1, a_1a_2a_3 > a_4a_1^2 + a_0a_3^2$. One can see that for a sufficiently small H: $a_n > 0$ ($n = 1, 2, 3, 4$), moreover

$$a_1a_2a_3 - a_4a_1^2 - a_0a_3^2 = mr_0^2(r_0 + m)R^2H^2/2 + O(H^3) > 0, \tag{40}$$

$$a_2a_3 - a_4a_1 = 2r_0^3 + O(H) > 0. \tag{41}$$

Thus, for small H the polynomial characteristic equation (39) has eigenvalues with only negative real parts and, consequently, the initial characteristic equation (37) also exhibits stability for small H. Note that stability is sustained in the case when we consider a parabolic approximation $r(h) \approx r_0 + Rh + R_1h^2$, where $R \neq 0$, $R_1 \neq 0$ (the need for considering such an approximation comes from the fact that in the second-order expansion (38), the quadratic term R_1 will be present. We should stress that here we are allowed to drop $O(H^3)$ and consider (39) since all the roots of (39) are perturbations of the solutions with $H = 0$ such that the maximal order of perturbation with respect to H does not exceed 2, i.e. it is less than 3 (we do not show the corresponding expressions $\lambda(H)$ of solutions of (39) for the sake of brevity).

Now let us suggest that for some critical $H > 0$, the stability of (37) changes and the real part of an eigenvalue becomes positive. This can occur at a Hopf bifurcation point, and the condition of stability change is $\lambda = ib$, where b is a positive real number. We substitute $\lambda = ib$ into the complex characteristic equation and obtain two

equations for its real and imaginary parts. After some re-arrangement, the equation for b becomes (see electronic Appendix 2 for the exact derivation)

$$-2\frac{\int_0^H r(h)\mathrm{d}h}{\int_0^H r^2(h)\mathrm{d}h}+\frac{\int_0^H \frac{r(h)\mathrm{d}h}{b^2+r^2(h)}}{\int_0^H \frac{r^2(h)\mathrm{d}h}{b^2+r^2(h)}}\left(1+\frac{b^2\int_0^H \frac{r(h)\mathrm{d}h}{b^2+r^2(h)}}{\int_0^H r(h)\mathrm{d}h}\right)+\frac{\int_0^H \frac{r(h)\mathrm{d}h}{b^2+r^2(h)}}{\int_0^H r(h)\mathrm{d}h}=0. \tag{42}$$

We substitute a particular parametrization $r(h)$ to verify whether or not (42) has a real value solution. In the case (42) does not have real solutions, the steady state of (6)–(7) will be always locally stable for $\beta = 0$ because for small H the eigenvalues always have nonzero negative real parts and for any $H > 0$, they will not vanish (otherwise we would have a solution with $\lambda = ib$, in which case b would solve (42)).

However, it is still an open question whether or not the equilibrium will remain stable for $\beta = 0$ for any arbitrary positive function $r(h)$. In our investigation, we checked several concrete families of ecologically relevant and mathematically tractable functions including linear, parabolic, cubic, exponential and sinusoidal functions given, respectively, by $r(h) = a_0 + a_1 h$, $r(h) = a_0 + a_2 h^2$, $r(h) = a_0 + a_3 h^3$, $r(h) = a_0 \exp(a_4 h)$ and $r(h) = a_0(1 + \epsilon \sin(\omega h))$, where a_i, ω, ϵ are parameters. For those functions, we can obtain analytical expressions for the corresponding integral and numerically check the possibility to find a solution of (42), by varying the parameters. For all these functions, we find that (42) has no real solution; thus, the equilibrium is always stable (we do not show the corresponding cumbersome expressions and graphs here for the sake of brevity).

3.2 Model 2: Local Growth Rate of Prey is Affected by Self-Shading

3.2.1 Existence of a Non-Trivial (Coexistence) Steady State

We look for the coexistence equilibrium (p_*, Z_*) of model (8)–(9). The steady-state equations read

$$r_0 \exp\left(-\int_0^h \nu p(h,t)\mathrm{d}h\right) = \alpha\frac{Z_*}{P_*}\frac{p_*(h)}{1+\beta p_*(h)}, \tag{43}$$

$$m = \frac{\alpha k}{P_* H}\int_0^H \frac{p_*^2(h)}{1+\beta p_*(h)}\mathrm{d}h, \tag{44}$$

$$P_* = \frac{1}{H}\int_0^H p_*(h)\mathrm{d}h. \tag{45}$$

From the first equation of the system, we obtain

$$\ln(r_0) - \nu\int_0^h p(h,t)\mathrm{d}h = \ln\left(\alpha\frac{Z_*}{P_*}\frac{p_*(h)}{1+\beta p_*(h)}\right). \tag{46}$$

We differentiate the above expression to obtain

$$-\nu = \frac{1}{p_*^2(h)(1+\beta p_*(h))} p_*'(h), \tag{47}$$

Integration of (47) gives

$$-\nu h + C = -\frac{1}{p_*(h)} + \beta \ln\left(\frac{1+\beta p_*(h)}{p_*(h)}\right), \tag{48}$$

where C is a constant of integration. The constant C can be found by setting $h = 0$ and using the expression for $p_*(0)$ from (43)

$$p_*(0) = \frac{P_* r_0}{\alpha Z_* - r_0 P_* \beta}, \tag{49}$$

After substituting C and some simplification, we obtain the expression for the stationary state $p_*(h)$:

$$-\nu h + \frac{r_0 P_* \beta - \alpha Z_*}{r_0 P_*} + \beta \ln\left(\frac{\alpha Z_*}{r_0 P_*}\right) = -\frac{1}{p_*(h)} + \beta \ln\left(\frac{1+\beta p_*(h)}{p_*(h)}\right), \tag{50}$$

The above expression is implicit since it is impossible to solve it analytically for $p_*(h)$ except in the particular case $\beta = 0$; however, from (47) one can conclude that $p_*(h)$ is a decreasing function of h. The maximal density through the column is attained at $h = 0$ and given by (49); the minimal density is achieved at $h = H$. From (43), we obtain the expression for $p_*(H)$

$$p_*(H) = \frac{P_* r_0 \exp(-H\nu P_*)}{\alpha Z_* - r_0 \exp(-H\nu P_*) P_* \beta}, \tag{51}$$

We use (51) and (50) to get the following relation between P_* and Z_*

$$0 = -\exp(P_* H \nu)\alpha Z_* + \beta P_*^2 H \nu + H \nu r_0 P_* + \alpha Z_*. \tag{52}$$

Next, we consider the stationary equation (44) for the predator and replace the integration variable h with $p(h)$ using (47).

$$\begin{aligned} m &= \frac{\alpha k}{P_* H} \int_0^H \frac{p_*^2(h)}{1+\beta p_*(h)} \mathrm{d}h = -\frac{\alpha k}{P_* H \nu} \int_{p_*(0)}^{p_*(H)} \frac{1}{(1+\beta p_*(h))^2} \mathrm{d}p \\ &= \frac{\alpha k}{P_* H \nu \beta} \left[\frac{1}{1+\beta p}\right]_{p_*(0)}^{p_*(H)}. \end{aligned} \tag{53}$$

We are allowed to make the above change of variables since $p(h)$ is a monotonically decreasing function. We substitute the values of $p_*(0)$ and $p_*(H)$ from (49) and (51), respectively, to obtain after simplification another identity linking P_* and Z_*

$$Z_* = \frac{(1 - \exp(-P_* H \nu))r_0 k}{m H \nu}. \tag{54}$$

Finally, we substitute the expression for Z_* from (54) into (52) to obtain the equation for P_* which reads

$$f(P_*) = \beta P_*^2 H \nu + P_* H \nu r_0 + \frac{\alpha k r_0}{m H \nu}(\exp(-P_* H \nu) - 1)(\exp(P_* H \nu) - 1) = 0, \tag{55}$$

This is a transcendental equation; however, we can make exhaustive conclusions about the existence of a positive solution of (55). At low P_*, the function $f(P_*)$ is linear and always has a positive slope. At large P_*, $f(P_*)$ becomes negative (the exponential term becomes dominant); thus, there should be at least one point where this function vanishes. Additionally, Eq. (55) should be considered together with the condition $p_*(h) > 0$, which is equivalent to $p_*(0) > 0$ since $p_*(h)$ is a decreasing function. From (49) and (54), it follows that the condition $p_*(0) > 0$ is equivalent to

$$f_1(P_*) = P_* \beta m H \nu + \alpha k \exp(-P_* H \nu) - \alpha k > 0, \tag{56}$$

It is easy to see that (56) will be satisfied for some $P_* > 0$ if and only if $\alpha k - \beta m > 0$. Further, by computing the second derivative of $f(P_*)$, one can show that for $\alpha k - \beta m > 0$, it is always negative; thus, there can be only one positive solution of (55). Hence, combining the above properties of $f(P_*)$ and $f_1(P_*)$, we find that the existence of the non-trivial steady state of the system (8)–(9) is given by the following

Proposition 3.5 *Model* (8)–(9) *admits a unique positive steady state* (p_*, Z_*) *in the case* $\alpha k - \beta m > 0$, *and the unique positive solution of* (55), *which would always exist under the mentioned condition, satisfies the inequality* (56).

It is easy to see that for $\beta \ll 1$, the conditions of the proposition are satisfied; thus, there always exists a non-trivial steady state. Let us consider a gradual increase in β while still keeping $\alpha k - \beta m > 0$. The root of $f(P_*) = 0$ will increase, whereas the root of $f_1(P_*) = 0$ will decrease. At a certain β_* both roots coincide, which is an unavoidable event since the root of $f_1(P_*) = 0$ will approach zero when $\alpha k = \beta m$. Thus, for all $\beta < \beta_*$, the system has a non-trivial coexistence equilibrium, whereas for $\beta > \beta_*$, a positive equilibrium is impossible. The exact value of β_* can be found from the condition $f(P_*) = f_1(P_*) = 0$ which results in a cumbersome analytical expression (not shown here).

3.2.2 Stability of the Non-Trivial (Coexistence) Steady State of Model 2

The linearization around the positive steady state (p_*, Z_*) of (8)–(9) results in a rather cumbersome characteristic equation. In this paper, we focus on an important particular case, where there is no saturation in the functional response of predator, i.e. $\beta = 0$. The linearized system becomes

$$\frac{\partial \Delta p}{\partial t}(h,t) = r_0 \exp\left(-\int_0^h \nu p_*(h)\mathrm{d}h\right)\left[\Delta p(h,t) - \nu p_*(h)\int_0^h \Delta p(x,t)\mathrm{d}x\right] - \alpha\left(\frac{p_*^2(h)}{P_*}\Delta Z(t) - \frac{p_*^2(h)Z_*}{P_*^2}\Delta P(t) + \frac{2Z_* p_*(h)}{P_*}\Delta p(h,t)\right), \quad (57)$$

$$\frac{\mathrm{d}\Delta Z}{\mathrm{d}t}(t) = -\frac{\alpha k Z_*}{H P_*^2}\Delta P(t)\int_0^H p_*^2(h)\mathrm{d}h + \frac{\alpha k Z_*}{H P_*}\int_0^H 2p_*(h)\Delta p(h,t)\mathrm{d}h. \quad (58)$$

We look for the solution in the form of $\Delta p(h,t) = w(h)\exp(\lambda t)$ and $\Delta Z(t) = U\exp(\lambda t)$. We substitute the expressions for the stationary solutions (48) ($\beta = 0$) and (54) to arrive at the following eigenvalue problem (W is the spatial average of w)

$$w(h)\lambda = \frac{Cr_0}{h\nu + C}\left[w(h) - \nu\frac{1}{h\nu + C}\int_0^h w(x)\mathrm{d}x\right] - \frac{Cr_0}{(h\nu + C)^2}\left(\frac{U}{Z_*} - \frac{W}{P_*} + 2(h\nu + C)w(h)\right), \quad (59)$$

$$U\lambda = \frac{kCr_0}{H}\left(-\frac{1}{P_*}W\int_0^H \frac{1}{(h\nu + C)^2}\mathrm{d}h + 2\int_0^H \frac{w(h)}{h\nu + C}\mathrm{d}h\right). \quad (60)$$

We re-arrange the first equation of the above system

$$w(h)\lambda(h\nu + C)^2 = -Cr_0(h\nu + C)w(h) - \nu Cr_0\int_0^h w(x)\mathrm{d}x - Cr_0\left(\frac{U}{Z_*} - \frac{W}{P_*}\right), \quad (61)$$

We differentiate both sides of (61) and obtain

$$\left(\frac{\mathrm{d}w}{\mathrm{d}h}(h\nu + C) + 2w(h)\nu\right)\lambda(h\nu + C) = Cr_0\left(-\nu w(h) - \frac{\mathrm{d}w}{\mathrm{d}h}(h\nu + C) - \nu w(x)\right) \quad (62)$$

After simplifying the above equation, we get

$$((h\nu + C)\lambda + \nu C)(h\nu + C)\frac{\mathrm{d}w}{\mathrm{d}h} = -2\nu w(h)((h\nu + C)\lambda + \nu C) \quad (63)$$

We suggest that $(h\nu + C)\lambda + \nu C \neq 0$ and derive the following equation for the eigenfunction $w(h)$

$$(h\nu + C)\frac{\mathrm{d}w}{\mathrm{d}h} = -2\nu w(h) \quad (64)$$

Integration of this linear equation gives the following eigenfunction

$$w(h) = \frac{1}{(h\nu + C)^2}. \quad (65)$$

Next, we substitute this function into system (59)–(60)

$$\lambda = -r_0 - Cr_0\left(\frac{U}{Z_*} - \frac{W}{P_*}\right), \tag{66}$$

$$U\lambda = \frac{kCr_0}{H}\left(-\frac{1}{P_*}W\int_0^H \frac{1}{(h\nu + C)^2}\mathrm{d}h + 2\int_0^H \frac{1}{(h\nu + C)^3}\mathrm{d}h\right), \tag{67}$$

where the value of W is obtained from

$$W = \frac{1}{H}\int_0^H w(h)\mathrm{d}h = \frac{1}{H}\int_0^H \frac{\mathrm{d}h}{(h\nu + C)^2} = \frac{1}{C(H\nu + C)}. \tag{68}$$

We simplify Eq. (67)

$$U\lambda = \frac{kr_0}{(h\nu + C)^2 C}\left(-\frac{1}{P_*} + 2C + H\nu\right), \tag{69}$$

finally, we substitute the expressions for the stationary value P_* into (66) and (69) to obtain the characteristic equation

$$0 = \lambda^2 + (1 - Q_1)r_0\lambda + Q_2, \tag{70}$$

where

$$Q_1 = \frac{H\nu}{(C + H\nu)\ln((C + H\nu)/C)} < 1, \tag{71}$$

$$Q_2 = \frac{kr_0}{(h\nu + C)^2 C Z_*}\left(-\frac{H\nu}{\ln((C + H\nu)/C)} + 2C + H\nu\right) > 0. \tag{72}$$

It is easy to see that characteristic equation (70) always has negative real parts; thus, the linearized system (57)–(58) is always stable.

We should also say that unlike the model without self-saturation, the number of eigenvalues is finite and there is a single eigenfunction. This can be explained by the fact that separation of variables provides us with only the solution for large values of time and does not describe transient regimes at small and intermediate times.

The above result can be summarized as the following

Theorem 3.6 *The steady state* (p_*, Z_*) *of model* (8)–(9) *is always locally asymptotically stable for* $\beta = 0$ *(Holling type I functional response).*

Remark 3.7 One can prove that in a similar way the stability of Eq. (57) governing the dynamics of prey for a constant (equilibrium) density of predator, i.e. for $Z(t) = const$ or $U(t) = 0$. The eigenvalue of the system is given by

$$\lambda = -(1 - Q_1)r_0 < 0. \tag{73}$$

This signifies that a spatial regrouping of the predator population (without variation in the total population size) alone can control the prey population in the case of self-shading.

4 Discussion and Summary of Results

In this paper, we revisit predator–prey interaction in ecosystems with a high nutrient load and explore the role that spatial heterogeneity of the environment and high predator mobility have in stability of such ecosystems. Our analytical investigations of the model predict that interplay between these two factors results in stabilization of an otherwise globally unstable predator–prey system. An important assumption for the realization of the given stabilization scenario is that the predator preferentially feeds at locations with high prey density [see relationship (4)]. Since spatial gradients in a species' growth rate across their habitats is a typical ecological situation, and many predators/consumers are highly mobile and feed mainly in patches of high food density (Milinski 1979; Godin and Keenleyside 1984; Lodge et al. 1988; Kacelnik et al. 1992; Begon et al. 2005; Nachman 2006) (see also Fig. 1 of the current paper), we claim here that the reported mechanism should be rather typical for marine, freshwater and terrestrial ecosystems under eutrophication. Our findings also provide a new and robust mechanism to resolve the famous 'paradox of enrichment', which is a long-standing enigma in theoretical ecology (Rosenzweig 1971; Gilpin 1972; Abrams and Walters 1996; Genkai-Kato and Yamamura 1999; Petrovskii et al. 2004; Mougi and Nishimura 2007; Roy and Chattopadhyay 2007).

Our models are formulated as integro-differential equations, which allows for the incorporation of different time scales: fast spatial movement of predator and slow population dynamics of both species. This makes the current framework more effective than classical reaction–diffusion models for modelling trophic interaction in small-sized habitats, since individuals cannot be assigned to a particular spatial location in this case while reaction–diffusion equations contain only local terms.

Here, we explore a generic predator–prey model with an infinitely large carrying capacity of prey (i.e. no resource limitation) and consider two main scenarios: (1) the prey growth rate gradient is fixed (Model 1), and the local growth rate of prey is affected by self-shading (Model 2). The main mathematical outcomes of our study are the following:

1. For each model (Models 1 and 2), we find the condition for the existence of the positive stationary state through which prey and predator can coexist for an arbitrary gradient of the growth rate $r(h) \geq 0$. Interestingly, including self-shading usually restricts the conditions of coexistence (cf. Propositions 3.1 and 3.5).
2. For Model 1, we have derived the general characteristic equation (34) governing the stability of the coexistence equilibrium. Using this equation, one can construct the Hopf bifurcation curve that separates stable and unstable dynamics without numerically integrating the underlying partial integro-differential equations (see an example below).
3. Analysis of the characteristic equation (34) shows that for a homogeneous environment, in which $r(h) \equiv const$, the system is always unstable provided there

is saturation in the functional response (Remark 3.4). Thus, spatial heterogeneity of the environment is a necessary condition for stability of the coexistence equilibrium.

4. For both Models 1 and 2, in the case of a linear (Holling type I) functional response of the predator, we analytically proved that the coexistence equilibrium is always stable. Since the system is structurally stable, the stability of the equilibrium is also guaranteed for sufficiently small $\beta > 0$, i.e. for a Holling type II functional response with low saturation.
5. Comparison of Models 1 and 2 shows that stabilization in the system with dynamical self-shading (Model 2) is potentially a stronger mechanism than the scenario, where the spatial gradient in the prey growth rate is fixed (Model 1). For instance, without saturation in the functional response ($\beta = 0$) the stabilization does not require changing the predator biomass: variation in the spatial distribution of a fixed number of predators can suppress the prey outbreak and re-establish the equilibrium (cf. Remarks 3.3 and 3.7).

In the case of a fixed prey growth rate gradient, the general characteristic equation (34) allows us to easily compute the Hopf bifurcation curve to direct numerical simulation of the underlaying integro-differential equations (6)–(7). As an illustrative example, here we have constructed the Hopf bifurcation curve for the system with a linear variation of the growth rate $r(h) = a_0 + a_1 h$ (see electronic Appendix 3 for detail). Figure 2 shows a set of bifurcation curves in the diagram a_1 and β constructed for a gradually increasing size H of the habitat. In each case, the stability region is located below the curve. One can see that increased the saturation in food consumption, signified by a large β, usually acts as a destabilizing factor, but the influence of the gradient of the growth rate a_1 is more complicated: small and large a_1 result in destabilization of the system, whereas stabilization occurs for some intermediate a_1. An increase in the size of the habitat can also either destabilize or stabilize the system. This result is somewhat counterintuitive since in earlier works it was shown that for an exponential parametrization of $r(h)$, an increase in the spatial gradient of the growth function or the size of the habitat will always facilitate stabilization of the system (Morozov et al. 2011; Lewis et al. 2013).

Our analytical investigation confirms the numerical results reported earlier in Morozov et al. (2011) and Lewis et al. (2013) about the possibility of the stabilization of systems with 'unlimited carrying capacity' and extend the previous findings to more general parametrizations of the spatial gradient of $r(h)$. In particular, we proved that for a small habitat size H, any arbitrary non-homogeneous dependence $r(h)$ will stabilize the predator–prey interactions (see Sect. 3.1.3). On the other hand, our work shows that using some other parametrizations, for example a linear function, can provide some qualitatively different prediction compared to the exponential dependence considered in Morozov et al. (2011) and Lewis et al. (2013). This underlines the danger of sticking to particular parametrizations when modelling predator–prey systems.

Throughout the paper, we have neglected the diffusion of the prey population by setting $D = 0$ in Eq. (1). Including diffusion $D > 0$ will make the model more realistic, but the equations become analytically untractable. Although one can still perform linearization techniques, it becomes impossible to obtain the resultant characteristic equation due to the presence of the second-order derivative with respect to x; thus, the

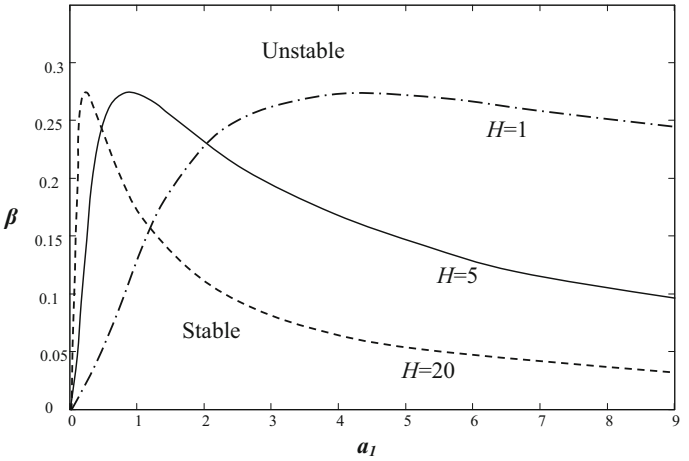

Fig. 2 Hopf bifurcation curves constructed for Model 1 (6)–(7) in the case the growth rate is a linear function of space $r(h) = a_0 + a_1 h$. The curves are plotted using the derived characteristic equation (34), for detail see Supplementary Appendix 3. Various curves are obtained for different size H of the habitat and each of them separates the stability region (*below the curve*) from the instability region (*above the curve*). The other model parameters are $m = 0.1$; $a_0 = 1$; $k = 1$; $= 2$

only way of exploring the system is by direct numerical simulation. For small values of D, the main conclusions of our paper obtained for $D = 0$ will hold due to the structural stability of the model equations. Interestingly, for some ecosystems (e.g. planktonic systems, Morozov et al. 2011; Lewis et al. 2013) the diffusion coefficient $D > 0$ is relatively small (compared to the interaction terms) so the results obtained should be close to those with $D = 0$. However, for a very large diffusion coefficient corresponding to a highly mobile prey, the system becomes homogeneous in space and is reduced to the classical Rosenzweig–MacArthur model, which is always globally unstable for any $\beta > 0$. Thus, the system will be destabilized for a certain critical D, which can be found numerically.

Finally, we should mention the open questions that our study raises. For instance, it would be an important extension to determine the stability or otherwise of the coexistence equilibrium of Model 1 in the case $r(h)$ is an arbitrary function for a Holling type I functional response [see Eq. (42)]. Based on preliminary results obtained for a small habitat size H, we hypothesize that for $\beta = 0$, the Model 1 should be stable for an arbitrary $r(h)$, but it remains to prove this conjecture rigorously. Another challenging issue is exploring the system stability for a more complicated relationship between $z(h, t)$ and $p(h, t)$, by taking into account possible interference between predators (Murdoch et al. 1992). For instance, this can be represented by setting $z(h) = \frac{p(h)^\mu}{P^\mu} Z$, $\mu > 0$ (Murdoch et al. 1992). Another interesting extension would be to investigate analytically the model combining self-shading of the population with a fixed gradient of local growth rate and combining Models 1 and 2. From the biological point of view, it might even be natural to consider situations when the growth function R (or r) can take negative values, i.e. the population of prey actually declines locally. In this more general case, model (6)–(7) will still be well posed, and solutions starting in

the positive cone would remain non-negative for all times. At the same time, equation (11) shows that there will be no strictly positive steady states of the model and this might influence the previous stability results. Models with locally negative growth rate of prey could therefore possess quite rich dynamics, and such models should definitely be a matter of further investigation.

Acknowledgments We thank the anonymous reviewer for his/her helpful comments and suggestions.

References

Abrams PA, Walters CJ (1996) Invulnerable prey and the paradox of enrichment. Ecology 77:1125–1133
Armstrong RA (1994) Grazing limitation and nutrient limitation in marine ecosystems: steady state solutions of an ecosystem model with multiple food chains. Limnol Oceanogr 39:597–608
Auger P, Lett C, Moussouai A, Pioch S (2010) Optimal number of sites in artificial pelagic multi-site fisheries. Can J Fish Aquat Sci 67:296–303
Bazykin A (1998) Nonlinear dynamics of interacting populations. World Scientific, River Edge
Begon M, Townsend CR, Harper JL (2005) Ecology: from individuals to ecosystems, 4th edn. Blackwell Publishing, London
Bollens SM, Frost BW (1989) Predator induced diel vertical migration in a marine planktonic copepod. J Plankton Res 11:1047–1065
Boyd PW (2002) Environmental factors controlling phytoplankton processes in the Southern Ocean. J Phycol 38:844–861
Briggs CJ, Hoopes MF (2004) Stabilizing effects in spatial parasitoid–host and predator–prey models: a review. Theor Popul Biol 65:299–315
Calsina Á, Farkas JZ (2012) Steady states in a structured epidemic model with Wentzell boundary condition. J Evol Equ 12:495–512
Chavez FP, Buck KR, Barber RT (1990) Phytoplankton taxa in relation to primary production in the equatorial Pacific. Deep Sea Res 37:1733–1752
Cottier FR, Tarling GA, Wold A, Falk-Petersen S (2006) Unsynchronised and synchronised vertical migration of zooplankton in a high Arctic fjord. Limnol Oceanogr 51:2586–2599
Cushing JM (1998) An introduction to structured population dynamics. SIAM, Philadelphia
Cullen JJ, Lewis MR, Davis CO, Barber RT (1992) Photosynthetic characteristics and estimated growth rates indicate that grazing is the proximate control of primary production in the equatorial Pacific. J Geophys Res 97:639–654
Farkas JZ, Hagen T (2007) Linear stability and positivity results for a generalized size-structured Daphnia model with inflow. Appl Anal 86:1087–1103
Farkas JZ, Hagen T (2009) Asymptotic analysis of a size-structured cannibalism model with infinite dimensional environmental feedback. Commun Pure Appl Anal 8:1825–1839
Farkas JZ, Morozov AY (2014) Modelling effects of rapid evolution on persistence and stability in structured predator–prey systems. Math Model Nat Phenom 9:26–46
Genkai-Kato M, Yamamura N (1999) Unpalatable prey resolves the paradox of enrichment. Proc R Soc Lond B 266:1215–1219
Gentleman W, Leising A, Frost B, Strom S, Murray J (2003) Functional responses for zooplankton feeding on multiple resources: a review of assumptions and biological dynamics. Deep Sea Res II.50(50):2847–2875
Gilpin ME (1972) Enriched predator–prey systems: theoretical stability. Science 177:902–904
Godin JGJ, Keenleyside MHA (1984) Foraging on patchy distributed prey by a cichlid fish, Teleostei, Cichlidae: a test of the ideal free distribution theory. Anim Behav 32:120–131
Holling CS (1959) The components of predation as revealed by a study of small-mammal predation of the European pine sawfly. Can Entomol 91:293–320
Jansen VAA (1995) Regulation of predator–prey systems through spatial interactions: a possible solution to the paradox of enrichment. Oikos 74:384–390
Jensen CXJ, Ginzburg LR (2005) Paradoxes or theoretical failures? The jury is still out. Ecol Model 188:3–14

Kacelnik A, Krebs JR, Bernstein C (1992) The ideal free distribution and predator–prey populations. Trends Ecol Evol 7:50–55

Lampert W (2005) Vertical distribution of zooplankton: density dependence and evidence for an ideal free distribution with costs. BMC Biol 3:10 (electronic)

Larsson P (1997) Ideal free distribution in Daphnia? Are daphnids able to consider both patch quality and the position of competitors? Hydrobiologia 360:143–152

Lewis ND, Morozov A, Breckels MN, Steinke M, Codling EA (2013) Multitrophic interactions in the sea: assessing the effect of infochemical-mediated foraging in a 1-d spatial model. Math Model Nat Phenom 8:25–44

Lodge DM, Barko JW, Strayer D, Melack JM, Mittelbach GG, Howarth RW, Menge B, Titus JE (1988) Spatial heterogeneity and habitat interactions in lake communities. In: Carpenter SR (ed) Complex interactions in lake communities. Springer, New York, pp 181–227

Milinski M (1979) An evolutionarily stable feeding strategy in sticklebacks. Z Tierpsychol 51:36–40

Morozov A, Arashkevich E, Nikishina A, Solovyev K (2011) Nutrient-rich plankton communities stabilized via predator–prey interactions: revisiting the role of vertical heterogeneity. Math Med Biol 28:185–215

Morozov AY, Pasternak AF, Arashkevich EG (2013) Revisiting the role of individual variability in population persistence and stability. PLoS ONE 8:e70576

Morozov AY, Petrovskii SP, Nezlin NP (2007) Towards resolving the paradox of enrichment: the impact of zooplankton vertical migrations on plankton systems stability. J Theor Biol 248:501–511

Mougi A, Nishimura K (2007) A resolution of the paradox of enrichment. J Theor Biol 248:194–201

Murdoch WW, Briggs CJ, Nisbet RM, Gurney WSC, Stewart-Oaten A (1992) Aggregation and stability in metapopulation models. Am Nat 140:41–58

Nachman G (2006) A functional response model of a predator population foraging in a patchy habitat. J Anim Ecol 75:948–958

Nisbet RM, Diehl S, Wilson WG, Cooper SD, Donalson DD, Kratz K (1997) Primary productivity gradients and short-term population dynamics in open systems. Ecol Monogr 67:535–553

Oaten A, Murdoch WW (1975) Functional response and stability in predator–prey systems. Am Nat 109:289–298

Ohman MD (1990) The demographic benefits of diel vertical migration by zooplankton. Ecol Monogr 60:257–281

Petrovskii S, Li B, Malchow H (2004) Transition to spatiotemporal chaos can resolve the paradox of enrichment. Ecol Complex 1:37–47

Poggiale J-C, Auger P (2004) Impact of spatial heterogeneity on a predator–prey system dynamics. C R Biol 327:1058–1063

Ryabov AB, Blasius B (2011) A graphical theory of competition on spatial resource gradients. Ecol Lett 14:220–228

Rosenzweig ML (1971) Paradox of enrichment: destabilization of exploitation ecosystems in ecological time. Science 171:385–387

Roy S, Chattopadhyay J (2007) The stability of ecosystems: a brief overview of the paradox of enrichment. J Biosci 32:421–428